

Two-Kaon Correlations in Central Pb + Pb Collisions at 158 A GeV/c

I. G. Bearden,¹ H. Bøggild,¹ J. Boissevain,² P. H. L. Christiansen,¹ L. Conin,³ J. Dodd,⁴ B. Erazmus,³ S. Esumi,⁵ C. W. Fabjan,⁶ D. Ferenc,⁷ A. Franz,⁶ J. J. Gaardhøje,¹ A. G. Hansen,¹ O. Hansen,¹ D. Hardtke,⁸ H. van Hecke,² E. B. Holzer,⁶ T. J. Humanic,⁸ P. Hummel,⁶ B. V. Jacak,⁹ K. Kaimi,^{5,*} M. Kaneta,⁵ T. Kohama,⁵ M. Kopytine,^{9,†} M. Leltchouk,⁴ A. Ljubičić, Jr.,⁷ B. Lörstad,¹⁰ N. Maeda,⁵ L. Martin,³ A. Medvedev,⁴ M. Murray,¹¹ H. Ohmishi,⁵ G. Paić,^{6,8} S. U. Pandey,⁸ F. Piuz,⁶ J. Pluta,³ V. Polychronakos,¹² M. Potekhin,⁴ G. Poulard,⁶ D. Reichhold,⁸ A. Sakaguchi,⁵ J. Schmidt-Sørensen,¹⁰ J. Simon-Gillo,² W. Sondheim,² T. Sugitate,⁵ J. P. Sullivan,² Y. Sumi,⁵ W. J. Willis,⁴ K. Wolf,^{11,*} N. Xu,² and D. S. Zachary⁸

(NA44 Collaboration)

¹Niels Bohr Institute, DK-2100 Copenhagen, Denmark

²Los Alamos National Laboratory, Los Alamos, New Mexico 87545

³Nuclear Physics Laboratory of Nantes, 44072 Nantes, France

⁴Department of Physics, Columbia University, New York, New York 10027

⁵Hiroshima University, Higashi-Hiroshima 739-8526, Japan

⁶CERN, CH-1211 Geneva 23, Switzerland

⁷Rudjer Bošković Institute, Zagreb, Croatia

⁸Department of Physics, The Ohio State University, Columbus, Ohio 43210

⁹State University of New York, Stony Brook, New York 11794

¹⁰Department of Physics, University of Lund, S-22362 Lund, Sweden

¹¹Cyclotron Institute, Texas A&M University, College Station, Texas 77843

¹²Brookhaven National Laboratory, Upton, New York 11973

(Received 17 April 2001; published 23 August 2001)

Two-particle interferometry of positive kaons is studied in Pb + Pb collisions at mean transverse momenta $\langle p_T \rangle \approx 0.25$ and 0.91 GeV/c. A three-dimensional analysis was applied to the lower p_T data, while a two-dimensional analysis was used for the higher p_T data. We find that the source-size parameters are consistent with the m_T scaling curve observed in pion-correlation measurements in the same collisions, and that the duration time of kaon emission is consistent with zero within the experimental sensitivity.

DOI: 10.1103/PhysRevLett.87.112301

PACS numbers: 25.75.Gz

Experimental studies of high-energy nuclear collisions at the BNL-AGS and CERN-SPS accelerators (beam energies from 10 to 200 GeV/nucleon) have revealed interesting features of hot and dense nuclear matter, and some characteristic signatures of a quark-gluon-plasma (QGP) phase have been reported [1]. If the hadronic source is formed in a first-order phase transition from a QGP phase in the course of collision, the hadronic expansion may slow down due to a softening of the equation of state. In such a case, a long duration time of particle emission is anticipated. Since a finite duration of particle emission increases the effective source size in the direction of particle velocity, and, since the shape of the two-particle correlation function is related to the effective source size, a difference between the widths of the peaks in the correlation functions in the direction of pair (“outward”) and perpendicular to it (“sideward”) might be a signature of QGP [2]. At SPS energies, systematic studies of particle correlations have been performed from $p + A$ to Pb + Pb collisions [3–7]. From the pion correlation studies in the Pb + Pb collisions, NA44 [5] reported that the two transverse radius parameters in the outward and sideward directions in the longitudinal center of mass system (LCMS) frame (see below) are

similar, implying no long duration time of emission. WA98 [6] measured the correlation function with the generalized Yano-Koonin parametrization and found the R_0 parameter, which reflects the duration of emission, is compatible with zero. While NA49 [7] observed a finite R_0 parameter in the Yano-Koonin-Podgoretskii parametrization to be approximately 3–4 fm/c, the value is small and not consistent with what would be expected from a strong first-order phase transition. All the experimental data support no long-lived intermediate hadron-parton mixed phase during the pion emission. There are discussions, however, that the pion-correlation functions might be distorted due to a large amount of decays from long-lived resonances, while kaon measurements can serve as a more sensitive probe of the space-time evolution [8–10]. The kaon duration time was measured in S + Pb collisions, but a long-lived mixed phase was also excluded by the data [4]. In this Letter, we present the first results of K^+K^+ correlations in central Pb + Pb collisions at the SPS energy and extract the duration time of the kaon emission.

The data were taken at the CERN-SPS with a 158 GeV/c per nucleon lead-ion beam incident on a lead target, using the NA44 spectrometer at two laboratory

angles: 44 and 131 mrad with respect to the beam axis. A description of the NA44 apparatus can be found elsewhere [4,5]. The lead beam was transported in vacuum up to a beam counter. The signal amplitude from the beam counter ensures a single lead ion impinging on the lead target at the entrance edge of the first dipole magnet. Behind the target, there were two multiplicity detectors characterizing each event. A set of scintillator bars was used primarily to generate a centrality trigger by measuring charged secondaries. A silicon pad detector with a full coverage in the azimuthal direction and segmented into 512 pads measured the $dN/d\eta$ distribution of charged particles in the pseudorapidity range between 1.5 and 3.3.

The secondary particles were transported to the tracking section through another dipole magnet and three quadrupole magnets. The quadrupole magnets control the three-dimensional momentum acceptance of the spectrometer. Two sets of quadrupole settings, referred to as the “horizontal” and “vertical” focus settings, were used. The horizontal (vertical) setting favors a wide momentum acceptance in the horizontal (vertical) space $p_x(p_y)$, and reduces the acceptance $p_y(p_x)$. In the discussion which follows, the direction with wide acceptance for a given mode (e.g., p_x for the horizontal mode) is referred to as the “favored” direction and the direction with narrow acceptance (e.g., p_y for the horizontal mode) is called “unfavored”. For the small angle measurements, collimators between the first dipole and the first quadrupole magnets further reduced the acceptance in the unfavored direction. These collimators reduced the number of particles in the acceptance without reducing the acceptance in the favored direction. The momentum settings of the spectrometer were 6 GeV/c for the small angle (low p_T) measurements and 7.5 GeV/c for the large angle (high p_T) measurements.

After the magnets, there were three tracking chambers (PC, SC1, SC2), three threshold-type gas Cherenkov counters (C1, C2, TIC), and three scintillator hodoscopes (H2, H3, H4). The pad chamber (PC) and the strip chambers (SC) provided precise hit position for the tracking algorithm. Although their position information was less precise, the hodoscopes were also used in track finding. C1 was the primary device for pion/kaon separation in the small angle measurements, while C2 and TIC were used for pion/kaon separation in the large angle measurements. Tracks were reconstructed by requiring hits in the tracking chambers and hodoscopes on straight lines. The three-dimensional momenta were calculated from the track information through a matrix, of which the elements were determined by a Monte Carlo simulation combined with the TURTLE code for the particle transportation through the magnetic field. Particle identification used time-of-flight information between the beam counter and the hodoscopes along with pulse height information from the Cherenkov counters. Figure 1 shows an example of such a plot

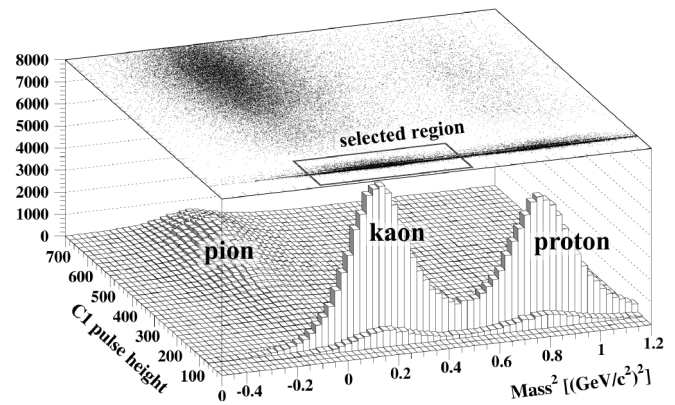


FIG. 1. The particle identification using the mass-squared and the C1 pulse height. Kaon and proton peaks are seen near the C1 pedestal (70 ch.), while a bump at around 600 ch. on C1 and $\text{mass}^2 \approx 0$ is of pion events accumulated with a hardware scaled-down trigger. On the top plane, a scatter plot is shown with the PID selection adopted in this analysis.

in the small angle measurements and also the particle-identification (PID) selection adopted in this analysis. Contaminations of pion and proton tracks in the kaon-identified pair samples were evaluated to be 0.15% and 3.9%, respectively. Therefore, contaminations of $\pi\pi$ and pp pairs in the KK samples were negligibly small.

At the small angle, the spectrometer covers the rapidity range of 2.9–3.3 with a p_T window below 0.6 GeV/c ($\langle p_T \rangle \approx 0.25$ GeV/c). The rapidity coverage in the large angle measurements is 2.4–2.9 with the p_T window of 0.7–1.4 GeV/c ($\langle p_T \rangle \approx 0.91$ GeV/c). Note that the colliding system is symmetric and the central rapidity is at 2.9, so the rapidity coverage in the high and low p_T measurements overlap well. The trigger required a lead ion in the beam counter, a large number of secondary particles in the scintillator bars, and at least two hits in hodoscopes H2 and H3. Off-line we required at least two kaons in each event and found the centrality of the lower p_T data set to be around 10% of the most central events while that of the high p_T sample was 18%.

The two-particle correlation function is defined by

$$C_{\text{raw}}(\vec{p}_1, \vec{p}_2) = \frac{P_2(\vec{p}_1, \vec{p}_2)}{P_1(\vec{p}_1)P_1(\vec{p}_2)} \approx \frac{\text{Real}(\vec{p}_1, \vec{p}_2)}{\text{Back}(\vec{p}_1, \vec{p}_2)}, \quad (1)$$

where the numerator is the joint probability of detecting two particles with momenta \vec{p}_1 and \vec{p}_2 , while the denominator is the product of the probabilities of detecting single particles with momenta \vec{p}_1 and \vec{p}_2 . The denominator was obtained by mixing two tracks picked up from two randomly selected different events. Ten mixed background pairs were generated for each real pair to reduce statistical uncertainties. There still remain several effects, which affect the true correlation function. The limited acceptance of the spectrometer distorts the real two-particle spectrum, and the finite momentum resolution smears the peak in

the correlation function. The repulsive Coulomb force separates particles of a pair going out at $\vec{p}_1 \approx \vec{p}_2$ and strongly suppresses the yield at $\vec{q} = \vec{p}_1 - \vec{p}_2 \sim 0$. The background two-particle spectrum generated by the event mixing method still contains effects of two-particle correlations, since a particle in a real event is always accompanied by another particle nearby in phase space. Since the degree of these effects depends on the strength of particle correlations of interest in a source, these effects were corrected through a Monte Carlo (MC) based iteration method. A C_2 function (described in the next paragraph) was assumed for a given set of source-size parameters (R 's and λ), and MC events were generated taking the spectrometer response into account. The wave integration method [11] was employed to simulate Coulomb effects in the finite source volume. The MC events were analyzed using exactly the same procedure as was applied to the experimental data. The correction factors to the C_{raw} function were evaluated by comparing the resultant MC correlation function with the given input C_2 function. The source-size parameters were deduced from the experimental correlation function after applying the correction factors to the C_{raw} function. The iteration ends when the extracted source-size parameters agree with the given parameters within an acceptable accuracy. The detailed procedure is described in the first article in Ref. [4] and more discussion can be found in Ref. [12].

After the PID selection and quality cuts, we have around 20×10^3 pairs in both the horizontal and vertical modes at the lower p_T , while 17×10^3 pairs in the horizontal mode at the higher p_T . A three-dimensional fit is applied to the lower p_T data. The observed momenta of each kaon pair are transformed to the LCMS, in which the momentum sum of two particles along the beam axis is zero, $\vec{p}_{z1} + \vec{p}_{z2} = 0$. The momentum variables of interest are defined in this system. The average momentum of the pair in the frame is $\vec{k}_T = (\vec{p}_{T1} + \vec{p}_{T2})/2$. Q_L is a projection of the momentum difference onto the beam axis, and Q_T is the momentum difference perpendicular to the beam axis. Q_T is further divided into two components. Q_{TO} is the component of Q_T along \vec{k}_T , and Q_{TS} is the component of Q_T perpendicular to both \vec{k}_T and the beam axis. The momentum resolution of Q_L , Q_{TO} , and Q_{TS} , including effects of multiple scattering in the target, were around 10, 20, and 20 MeV/c, respectively. The correlation functions C_2 in both the horizontal and vertical modes are simultaneously fitted using the maximum likelihood method with

$$C_2(Q_{TO}, Q_{TS}, Q_L) = D(1 + \lambda e^{-Q_{TO}^2 R_{TO}^2 - Q_{TS}^2 R_{TS}^2 - Q_L^2 R_L^2}), \quad (2)$$

where λ is a factor introduced to express chaoticity of quantum states of the source and R 's are variables representing multidimensional radii of the system in question. D is a free parameter for normalization in each mode. A two-dimensional equation replacing

TABLE I. Fit results of Gaussian parametrizations of the K^+K^+ correlation functions at low and high p_T . The errors are statistical and systematical ones.

$\langle p_T \rangle$ [GeV/c]	0.25	0.91
λ	$0.84 \pm 0.06 \pm 0.07$	$0.61 \pm 0.20 \pm 0.16$
R_L [fm]	$4.36 \pm 0.33 \pm 0.32$	$3.20 \pm 0.54 \pm 0.45$
R_T [fm]	n/a	$3.59 \pm 0.67 \pm 0.97$
R_{TS} [fm]	$4.04 \pm 0.28 \pm 0.32$	n/a
R_{TO} [fm]	$4.12 \pm 0.26 \pm 0.31$	n/a
$\chi^2/\text{d.o.f.}$	5139/2978	117/107

$-Q_{TO}^2 R_{TO}^2 - Q_{TS}^2 R_{TS}^2$ in Eq. (2) with $-Q_T^2 R_T^2$ is employed to fit the correlation function in the horizontal mode at the higher p_T . The fit results are given in Table I, where the systematic uncertainties reflect the effect of (i) cut parameters to define a track, (ii) cut parameters to select pairs, (iii) momentum resolution, (iv) two-track resolution, (v) momentum distribution of particle production in MC, and (vi) fitting to finite bins. Figure 2 shows projections of the correlation function onto each axis of the momentum difference where the projection is over the lowest 40 MeV/c of the other directions in the momentum difference. In these plots, the solid lines show the results of fit projected in the same way as the data.

The three source-size parameters (R_L , R_{TO} , R_{TS}) in the three-dimensional fit are quite similar to each other—as was observed in pion correlation measurements in the same colliding system [5]. Since R_{TS} and R_L represent the geometric information of the source most directly, they are compared in Fig. 3 with those of pions. The present data at $m_T \approx 0.55 \text{ GeV}/c^2$ seems to stay on the m_T scaling

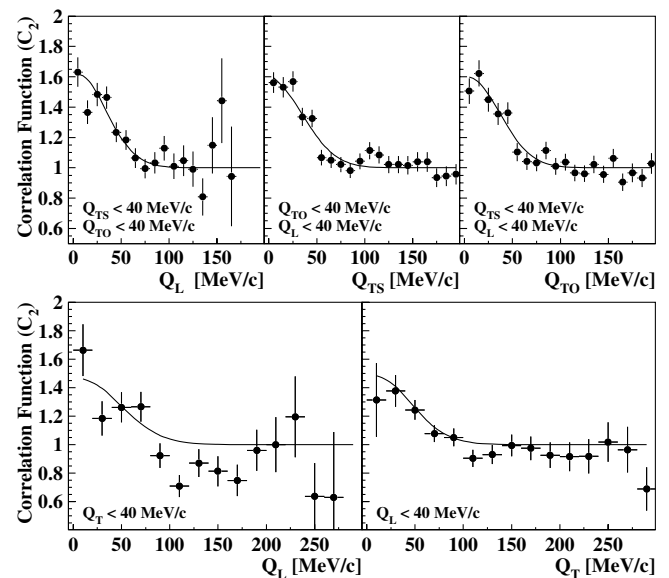


FIG. 2. Projections of the K^+K^+ correlation functions at $p_T \approx 0.25 \text{ GeV}/c$ (top) and $p_T \approx 0.91 \text{ GeV}/c$ (bottom). The solid lines show the projections of the fit with the Gaussian parametrization.

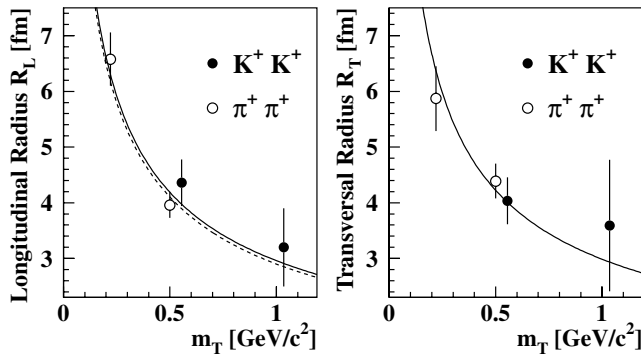


FIG. 3. The longitudinal and transversal source-size parameters of K^+K^+ at $p_T \approx 0.25$ and 0.91 GeV/ c (solid circles), compared with those of pions (open circles). The dashed curve shows a fit to $R = A/\sqrt{m_T}$ for pions, while the solid curve is the fit to the pion and kaon data points in each plot.

curve (dashed line) which came from the pion correlation measurements. To confirm this tendency, we put R_T and R_L from the two-dimensional fit at the higher p_T ($m_T \approx 1.0$ GeV/ c^2) on the same plot. They also seem consistent with the scaling curve. A fit to the four data points in each plot with a single scaling curve, $R = A/\sqrt{m_T}$, gives $A = 3.0 \pm 0.2$ fm GeV $^{1/2}$ c^{-1} in both cases as shown with solid curves.

The dependences on m_T are predicted with models including hydrodynamical expansion in a source [13–15]. The experimental radius parameters are interpreted as a length of homogeneity which is in turn dependent on a geometrical source-size R_{geom} and a thermal length R_{therm} . The “boost invariant expansion” along the longitudinal direction leads to an expression $R_L = \tau\sqrt{T_0/m_T}$, ignoring the contribution from R_{geom} . Assuming a freeze-out temperature T_0 of 100–140 MeV, we could extract the freeze-out time τ from the present A parameter to be 7–10 fm/ c , which is in good agreement with the WA98 [6] and NA49 [7] results. In a hydrodynamic model under certain conditions [15], one can derive an analytic expression for the radii $R_T \approx R_L \approx \tau\sqrt{T_0/m_T}$. Our data are consistent with such a scenario. The common m_T scaling for pions and kaons may imply that thermal freeze-out occurs simultaneously for both pion and kaons and that therefore they receive a common Lorentz boost. This is consistent with the hydrodynamic hypothesis. A similar conclusion can be drawn from the linear increase of the single particle inverse slopes with mass [16].

We derived the duration time $\Delta\tau$ of kaon emission from the quadratic difference of R_{T0} and R_{TS} in Eq. (2) as $\Delta\tau = \sqrt{R_{T0}^2 - R_{TS}^2}/\beta$, where β is the transverse ve-

locity of the kaon pair in the LCMS frame. We find $\Delta\tau = 2.2 \pm 5.2(\text{stat}) \pm 6.1(\text{syst})$ fm/ c . The kaon duration time is short and similar to those observed for pions in the same colliding system and for kaons in the S + Pb collisions. The present result excludes simple scenarios of a prolonged mixed phase anticipated in a first-order phase transition from a QGP phase.

The NA44 collaboration wishes to thank the staff of the CERN PS-SPS accelerator complex for their excellent work. We are also grateful for support given by the Danish Natural Science Research Council; the Japanese Society for the Promotion of Science; the Ministry of Education, Science and Culture, Japan; the Swedish Science Research Council; the Austrian Fond für Förderung der Wissenschaftlichen Forschung; the National Science Foundation, and the U.S. Department of Energy.

*Deceased.

†On an unpaid leave from P.N. Lebedev Physical Institute, Russian Academy of Sciences.

- [1] E.g., see *Proceedings on Quark Matter 1999*, edited by L. Riccati, M. Maserà, and E. Vercellin [Nucl. Phys. A **661**, 1c–765c (1999)]; S. A. Bass *et al.*, J. Phys. G **25**, R1 (1999).
- [2] G. Bertsch and G. E. Brown, Phys. Rev. C **40**, 1830 (1989); S. Pratt, Phys. Rev. D **33**, 1314 (1986).
- [3] NA35 Collaboration, A. Bamberger *et al.*, Phys. Lett. B **203**, 320 (1988); T. Alber *et al.*, Z. Phys. C **66**, 77 (1995).
- [4] NA44 Collaboration, H. Boggild *et al.*, Phys. Lett. B **302**, 510 (1993); **349**, 386 (1995); H. Baker *et al.*, Z. Phys. C **64**, 209 (1994); Phys. Rev. Lett. **74**, 3340 (1995); K. Kaimi *et al.*, Z. Phys. C **75**, 619 (1997).
- [5] NA44 Collaboration, I. G. Bearden *et al.*, Phys. Rev. C **58**, 1656 (1998); Eur. Phys. J. C **18**, 317 (2000).
- [6] WA98 Collaboration, M. M. Aggarwal *et al.*, Eur. Phys. J. C **16**, 445 (2000).
- [7] NA49 Collaboration, H. Appelshäuser *et al.*, Eur. Phys. J. C **2**, 661 (1998).
- [8] M. Gyulassy and S. S. Padula, Phys. Rev. C **41**, R21 (1990).
- [9] J. Bolz *et al.*, Phys. Rev. D **47**, 3860 (1993).
- [10] U. A. Wiedemann and U. Heinz, Phys. Rev. C **56**, 3265 (1997).
- [11] S. Pratt, Phys. Rev. D **33**, 72 (1986).
- [12] W. A. Zajc *et al.*, Phys. Rev. C **29**, 2173 (1984).
- [13] S. V. Akkelin and Yu. M. Sinyukov, Phys. Lett. B **356**, 525 (1995).
- [14] U. A. Wiedemann, P. Scotto, and U. Heinz, Phys. Rev. C **53**, 918 (1996).
- [15] T. Csörgő and B. Lörstad, Phys. Rev. C **54**, 1390 (1996).
- [16] I. G. Bearden *et al.*, Phys. Rev. Lett. **78**, 2080 (1997).